UV Irradiation-Induced Shell Cross-Linked Micelles with pH-Responsive Cores Using ABC Triblock Copolymers

Xiaoze Jiang,[†] Shizhong Luo,[†] Steven P. Armes,[‡] Wenfang Shi,[†] and Shiyong Liu*[,†]

Department of Polymer Science and Engineering, and Hefei National Laboratory for Physical Sciences at Microscale, University of Science and Technology of China, Hefei, 230026, Anhui Province, P. R. China, and Department of Chemistry, University of Sheffield, Brook Hill, Sheffield, South Yorkshire, S3 7HF, U.K.

Received June 21, 2006; Revised Manuscript Received July 10, 2006

ABSTRACT: A triblock copolymer, poly(ethylene glycol)-*b*-poly(glycerol monomethacrylate)-*b*-poly(2-(diethylamino)ethyl methacrylate) (PEG−PGMA−PDEA), was synthesized via atom transfer radical polymerization (ATRP) by successive polymerization of glycerol monomethacrylate (GMA) and 2-(diethylamino)ethyl methacrylate (DEA) using a PEG-based ATRP macroinitiator. Reacting the obtained triblock copolymer with varying amounts of cinnamoyl chloride in anhydrous pyridine yielded PEG−(PCGMA-*co*-PGMA)−PDEA triblock copolymer with photo-cross-linkable moieties, where PCGMA is poly(3-cinnamoyl glycerol monomethacrylate) and the mean degree of cinnamoylation ranges from 5 to 50 mol % relative to the PGMA block. All PEG−(PCGMA-*co*-PGMA)−PDEA triblock copolymers molecularly dissolve in aqueous media at acidic pH; upon addition of NaOH, micellization occurred above pH 7−8 to form three-layer "onionlike" micelles comprising PDEA cores, PCGMA-*co*-PGMA inner shells, and PEG outer coronas. The pH-induced micellization kinetics of PEG_{113}−$(CGMA_{0.5}$-*co*-$GMA_{0.5})_{50}$−DEA_{65} triblock copolymers was investigated by stopped-flow light scattering upon a pH jump from 3 to 10, and compared to that of PEG_{113}−$PGMA_{50}$−$PDEA_{65}$. Facile cross-linking of the PCGMA-*co*-PGMA inner shell was then conducted via UV irradiation. The PDEA cores of the resulting shell cross-linked (SCL) micelles exhibited reversible pH-responsive behavior. The extent of pH-induced swelling/shrinking and the colloidal stability of SCL micelles were mainly determined by the extent of cross-linking. The dissociation kinetics of the triblock copolymer micelles before and after shell cross-linking was also investigated employing the stopped-flow technique. It was found that SCL micelles prepared at higher degrees (>20 mol %) of cross-linking exhibited excellent colloidal stability to external pH changes.

Introduction

Following the pioneering work by Wooley and co-workers in 1996, there has been increasing interest in shell cross-linked (SCL) micelles.[1,2] These fascinating supramolecular structures combine the properties of micelles, microgels, nanoparticles, and dendrimers, and various applications such as targeted drug delivery, sequestration of metabolites and entrapment of environment pollutants have been subsequently suggested.[3−9] In particular, recent efforts have focused on the synthesis of SCL micelles that have either hollow SCL micelles[4,10,11] or tunable hydrophilic cores.[12−15] In principle, hollow SCL micelles offer larger loading capacities, but tunable hydrophilic cores are also attractive since no core removal step is required, and there is the potential for the triggered release of encapsulated actives via various chemical stimuli such as pH, temperature, ionic strength, etc.

The synthesis of well-defined block copolymers generally requires either living or pseudo-living polymerization chemistry. Given the stringent purification protocols that are required for ionic polymerization, increasing attention is now being given to the use of atom transfer radical polymerization (ATRP)[16,17] for the preparation of the block copolymer precursors utilized in the synthesis of SCL micelles.[5,12,18−20] We have developed ATRP for the efficient polymerization of hydrophilic monomers in alcoholic media at room temperature,[21−26] and demonstrated that ABC triblock copolymers offer great advantages over conventional AB diblock copolymers, since the former allow inner-shell cross-linking to be carried out at relatively high solids (10 wt %) with negligible intermicellar cross-linking.[27]

The cross-linking strategies described in the literature have certain limitations. For example, Wooley's group[1,2] use carbodiimide coupling chemistry to link carboxylic acid groups via diamines. Obvious disadvantages here are the cost of the reagents and time-consuming cleanup procedures (typically involving dialysis). Other cross-linking approaches include reacting the *N*,*N*′-acryloxysuccinimide (NAS) or tertiary-amine-containing block with bifunctional cross-linking agents such as diamines[28−30] or 1,2-bis(2-iodoethoxy)ethane (BIEE),[13,14,21,31−33] respectively. Divinyl sulfone (DVS) can also be employed as the cross-linking agent for hydroxyl-containing block copolymers.[25] However, DVS is readily hydrolyzed (slowly at neutral pH but more rapidly in alkaline media) and dialysis is again needed to remove small molecule side-products. Liu and coworkers [9,11,31,34] prefer the UV-induced coupling of cinnamate groups to obtain stable core or shell cross-linked micelles, mostly in organic solvents. If commercial applications of SCL micelles are to be realized, the cross-linking chemistry should ideally be nontoxic, cost-effective, and facile under mild conditions (e.g., aqueous solution and ambient temperature) and should not produce any small molecule byproducts.

In principle, the combination of photo-cross-linking chemistry of cinnamate groups with *hydrophilic* ABC triblock copolymers, while maintaining the water solubility of the cinnamate-based inner shell, should be a useful new route for the preparation of SCL micelles in aqueous media. Herein we describe the facile

* To whom correspondence should be addressed. E-mail: sliu@ustc.edu.cn.
[†] Department of Polymer Science and Engineering, and Hefei National Laboratory for Physical Sciences at Microscale, University of Science and Technology of China.
[‡] Department of Chemistry, University of Sheffield.

10.1021/ma061386m CCC: $33.50
Published on Web 08/03/2006

preparation of SCL micelles with pH-responsive cores from poly(ethylene glycol)-*b*-poly(glycerol monomethacrylate)-*b*-poly(2-(diethylamino)ethyl methacrylate) (PEG−PGMA−PDEA). Mono-esterification of up to 50% of the GMA residues with cinnamoyl chloride can be achieved while maintaining the water solubility of the copolymer chains. The triblock copolymer precursor was synthesized via ATRP, and then partially esterified to produce a PCGMA-*co*-PGMA middle block with differing molar contents of poly(3-cinnamoyl glycerol monomethacrylate) (PCGMA). The pH-induced micellization and subsequent UV-induced cross-linking of the copolymer chains by the [2 + 2] cycloaddition of the cinnamate groups was then studied. The pH-induced micellization and dissociation kinetics prior to shell cross-linking and the rate of the micelle swelling after cross-linking were also investigated using the stopped-flow light scattering technique.

Experimental Section

Materials. Monohydroxy-capped poly(ethylene glycol) (PEG_{113}−OH) with a mean degree of polymerization, DP, of 113 (M_n = 5000 g/mol, M_w/M_n = 1.10) was purchased from Fluka and dried at 30 °C under vacuum overnight prior to use. Glycerol monomethacrylate (GMA) was kindly donated by Cognis Performance Chemicals (Hythe, U.K.). 2-(Diethylamino)ethyl methacrylate (DEA, Aldrich, 98%) and GMA monomers were passed through basic alumina columns to remove inhibitor and then vacuum distilled from CaH_2 and stored at −20 °C prior to use. The Cu(I)-Cl catalyst, 2,2'-bipyridine(bpy) ligand, 2-bromoisobutyryl bromide, and cinnamoyl chloride were all purchased from Aldrich and used without further purification. Other reagents were purified according to standard procedures.

Preparation of PEG_{113}—Br Macroinitiator. In a typical example, PEG_{113}−OH (30.0 g, 0.006 mol) was dissolved in 300 mL of dry toluene in a 500 mL three-neck flask. After azeotropic distillation of 30−40 mL of toluene at reduced pressure to remove traces of water, triethylamine (1.7 mL, 0.012 mol) was added and the solution mixture was cooled to 0 °C. Then 2-bromoisobutyryl bromide (1.5 mL, 0.012 mol) was added dropwise via syringe over 1 h and the reaction mixture was stirred at room temperature overnight. The stirred solution was treated with charcoal, which was subsequently removed by filtration, and most of the toluene was removed by rotary evaporation prior to precipitation into a 10-fold excess of ether. The crude polymer was dried under vacuum, dissolved in water at pH 8−9, and then extracted with dichloromethane. The organic layers were collected and dried over $MgSO_4$, and removal of the solvent under vacuum led to isolation of the purified macroinitiator (PEG_{113}−Br). ^{1}H NMR studies in D_2O (δ = 1.84 (6 *H*), δ = 3.56 (451 *H*)) indicated that the terminal hydroxyl group on the PEG_{113}−OH precursor was fully esterified.

Preparation of PEG—PGMA—PDEA Triblock Copolymer. A reaction flask with a magnetic stirrer and a rubber septum was charged with PEG_{113}−Br macroinitiator (2.0 g, 4×10^{-4} mol) and GMA (3.33 g, 0.0208 mol) and methanol (3.0 mL). The flask was degassed by three freeze−pump−thaw cycles, and then $Cu^{I}Cl$ and 2, 2'-bipyridine(bpy) were added to the reaction flask to start the polymerization under a N_2 atmosphere at room temperature. After the GMA conversion had reached more than 95% (as judged by ^{1}H NMR), degassed DEA monomer in methanol was then added to the reaction flask via a double-tipped needle. The reaction solution became dark green and more viscous as the second-stage polymerization proceeded. After 15 h, the conversion was close to 98% as judged by ^{1}H NMR spectroscopy and the polymerizing solution was quenched in liquid nitrogen. The reaction mixture was diluted with methanol and passed though a silica gel column to remove the copper catalyst. After evaporation of all the solvent, drying in a vacuum oven at room temperature yielded a colorless copolymer. DMF GPC analyses of the PEG−PGMA−PDEA triblock copolymer precursor revealed symmetric, monomodal trace that clearly shifted to higher molecular weight as compared to that of the PEG−PGMA diblock copolymer. The M_n of the PEG−PGMA−PDEA triblock copolymer determined by GPC relative to polystyrene standards was 39 000 g mol^{-1}, and the M_w/M_n is 1.23. The actual degrees of polymerization (DP) of PGMA and PDEA blocks were calculated to be 50 and 65, respectively, from the ^{1}H NMR spectrum.

Preparation of PEG—(PCGMA-*co*-PGMA)—PDEA Triblock Copolymer. The PGMA middle block of the PEG−PGMA−PDEA triblock copolymer precursor was converted to a PCGMA-*co*-PGMA block, where PCGMA denotes poly(3-cinnamoyl glycerol monomethacrylate) with the molar content of 3-cinnamoyl glycerol monomethacrylate (CGMA) residues in the middle block ranges from 5 to 50 mol % by reacting varying amounts of cinnamoyl chloride in dry pyridine overnight at room temperature.[11,31] In a typical example for the synthesis of PEG−(PCGMA-*co*-PGMA)-PDEA with the molar content of CGMA residues in the middle block being 50 mol %, the PEG−PGMA−PDEA triblock copolymer (0.44 g, 0.88 mmol GMA residues) was dissolved in 10 mL of dry pyridine in a 50 mL flask. Then cinnamoyl chloride (0.0732 g, 0.44 mmol) was added and the reaction mixture was stirred at room-temperature overnight. The solution was then filtered to remove pyridinium salt and the filtrate was precipitated into excess *n*-hexane. The crude product was redissolved in DMF and precipitated into ether for 3 times prior to drying in a vacuum oven at room-temperature overnight to obtain a white powder in ∼90% yield. The degree of esterification was determined to be ∼49 mol %, from the ^{1}H NMR spectrum by integrating the signals of the cinnamate group at δ 7.2−7.6 ppm vs the signals of the PGMA at δ 3.7−4.2 ppm, indicating that the mono-esterification of the GMA residues is almost quantitative based on the feed ratio of cinnamoyl chloride to the GMA residues. The modified triblock copolymer was denoted PEG_{113}−$(PCGMA_x$-*co*-$PGMA_{1-x})_{50}$−$PDEA_{65}$, where *x* indicates the molar content of CGMA residues in the middle block. Considering that every GMA residue has two hydroxyl groups, the extent of esterfication of the hydroxyl groups of PCGMA block is *x*/2. A series of triblock copolymers with different *x* were prepared by varying the amount of cinnamoyl chloride in the feed ratio.

Preparation of Aqueous Solutions of Micelles and SCL Micelles. The PEG−(PCGMA-*co*-PGMA)−PDEA triblock copolymers with different PCGMA molar contents were molecularly dissolved at pH 3 using HCl and the solution pH was adjusted to pH 10 with concentrated NaOH so as to induce micelle formation at the final copolymer concentration of 1.0 g/L. The aqueous micellar solution was subjected to UV irradiation using a 1 kW mercury lamp (LT-UV102, made by Lantian company, Beijing), which had characteristic emission wavelengths ranging from 260 to 290 nm. Conversion of the cinnamate double bonds was monitored by monitoring the reduction of the absorbance at 274 nm, which is characteristic of the cinnamate group, using a Perkin-Elmer Lamba array 3840 instrument.[11]

Characterization. Molecular weight distributions were assessed by gel permeation chromatography (GPC) in DMF containing 1.0 g/L LiBr at a flow rate of 1.0 mL min^{-1} using a series of two linear Styragel columns (HT3, HT4), a Waters 1515 pump and waters 2414 differential refractive index detector (set at 30 °C) and an oven temperature of 60 °C. Calibration was performed using a series of near-monodisperse polystyrene standards.

Transmission electron microscopy (TEM) images were recorded using a Philips CM120 electron microscope at an accelerating voltage of 200 kV. TEM samples were prepared by placing dilute aqueous solutions (1 g/L) of SCL micelles at pH 3 on copper grids coated with thin films of Formvar and carbon. No staining was required.

All ^{1}H NMR spectra were recorded in D_2O or *d*-methanol using a Bruker 300 MHz spectrometer. FT-IR spectra were recorded on a Galaxy series 4030 instrument (Mattson) using Win FIRST V2.10 software. The spectra were collected at 64 scans with a spectral resolution of 4 cm^{-1}.

A commercial spectrometer (ALV/DLS/SLS-5022F) equipped with a multitaudigital time correlation (ALV5000) and a cylindrical

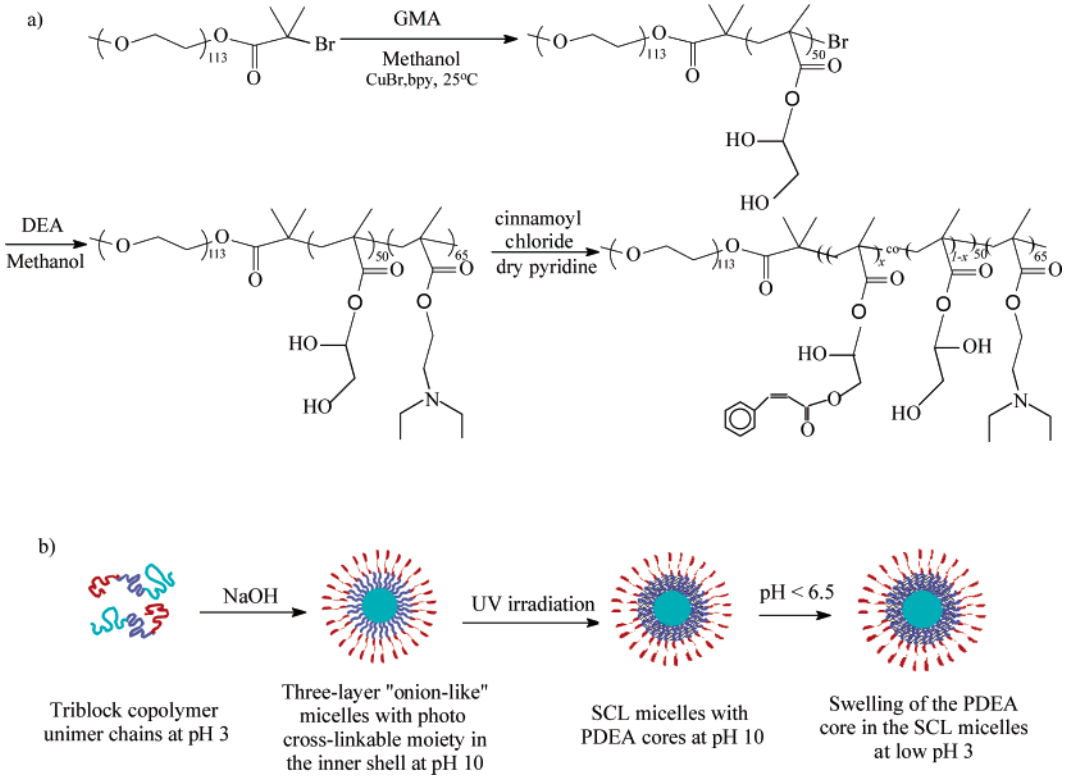

Figure 1. (a) Reaction scheme for the synthesis of the $PEG_{113}-PGMA_{50}-PDEA_{65}$ precursors and final $PEG_{113}-(PCGMA_x\text{-}co\text{-}PGMA_{1-x})_{50}-PDEA_{65}$ triblock copolymers. (b) Schematic illustration of the formation of three-layer onionlike micelles and shell cross-linked (SCL) micelles with pH responsive cores from the $PEG_{113}-(PCGMA_x\text{-}co\text{-}PGMA_{1-x})_{50}-PDEA_{65}$ triblock copolymers.

22 mW Uniphase He−Ne laser ($\lambda_0 = 632$ nm) was used for laser light scattering studies. In dynamic light scattering (DLS), the Laplace inversion of each measured intensity−intensity−time correlation function $G^{(2)}(q,t)$ in the self-beating mode can lead to a line-width distribution $G(\Gamma)$. For a pure diffusive relaxation, Γ is related to the translational diffusion coefficient D by $(\Gamma/q^2)_{C\to 0,q\to 0\to D}$, or further to the hydrodynamic radius, R_h, by the Stokes−Einstein equation, $R_h = (k_B T/6\pi\eta_0)/D$, where k_B, T, and η_0 are the Boltzmann constant, the absolute temperature, and the solvent viscosity, respectively

Stopped-flow studies were carried out using a Bio-Logic SFM 300/S stopped-flow instrument. The SFM-300/*S* is a three-syringe (10 mL) instrument in which all step-motor-driven syringes (S1, S2, and S3) can be operated independently to conduct either single-mixing or double-mixing experiments. The SFM-300/S stopped-flow device is attached to a MOS-250 spectrometer; kinetic data were fitted using the Biokine program supplied by the manufacturer (Bio-Logic, France). For light scattering detection at a scattering angle of 90°, both the excitation and emission wavelengths were adjusted to 330 nm with 10 nm slits. The FC-08 and FC-15 flow cells give typical dead times of 1.1 and 2.6 ms, respectively.

Results and Discussion

PDEA homopolymer is a weak polybase with a pK_a of ~7.3.[35−38] It is water-insoluble at neutral or alkaline pH; while below pH 7, it is molecularly soluble as a weak cationic polyelectrolyte due to protonation of its tertiary amine groups. At room temperature, the PEG and PGMA blocks are water-soluble over the entire pH range. The synthesis of PEG−PGMA−PDEA triblock copolymer via ATRP in methanol at room-temperature had been described in detail previously.[25,30] A general reaction scheme for the syntheses of the PEG−PGMA−PDEA triblock copolymer and the subsequent partial esterification with cinnamoyl chloride is shown in Figure 1a.

The cross-linkable cinnamate group has been widely utilized in the photolithography industry.[34] It is both nontoxic and cost-effective and its cross-linking chemistry is facile under mild conditions, producing no small molecule byproducts.[39] However, the cinnamate group is rather hydrophobic and hence normally water-insoluble. Fortunately, PGMA homopolymer partially esterified with cinnamoyl chloride remains water-soluble, provided that the extent of mono-esterification is less than 50%. Thus, the PEG−PGMA−PDEA triblock copolymer was esterified to give PEG−(PCGMA-*co*-PGMA)−PDEA by reacting the GMA residues with varying amounts of cinnamoyl chloride. Because the secondary hydroxyl groups in the GMA residues are less reactive than the primary hydroxyl groups due to steric hindrance, and the hydroxyl groups are in excess relative to that of cinnamoyl chloride, on average the GMA units are presumably mono-esterified even at an extent of esterification of 50 mol % relative to the GMA residues. The molar contents of PCGMA in the middle block are given by x = [CGMA]/([CGMA]+ [GMA]) × 100%, the mono-esterification of the GMA units can be carried out in a quantitative manner, as judged from the target degree of esterification and that calculated from ^{1}H NMR. The molar contents of CGMA units in the middle block were kept to be below 50 mol % to preserve its water solubility. DLS measurements on these esterified triblock copolymers (x ranges from 5 to 50 mol %) at pH 3 revealed intensity-average hydrodynamic diameters, $\langle D_h \rangle$, of ~ 7−9 nm with very low scattering intensities. This indicated that the triblock copolymers were molecularly dissolved in acidic conditions.

pH-Induced Formation of Three-Layer "Onion-Like" Micelles. On addition of NaOH to dilute acidic solutions of either PEG−(PCGMA-*co*-PGMA)−PDEA or PEG-GMA-DEA triblock copolymer, micellization occurred above pH 7−8, as indicated by the bluish tinge that is characteristic of micellar solutions. DLS studies revealed narrow, monomodal size distributions in all cases. For $PEG_{113}-(PCGMA_x\text{-}co\text{-}PGMA_{1-x})_{50}-$

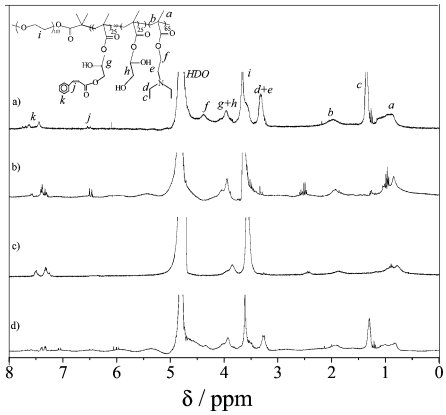

Figure 2. ^{1}H NMR spectra of the $PEG_{113}-(PCGMA_{0.5}\text{-}co\text{-}PGMA_{0.5})_{50}-PDEA_{65}$ triblock copolymer: (a) at pH 3; (b) at pH 10; (c) after UV irradiation at pH 10 for 10 min; (d) at pH 3 after shell cross-linking.

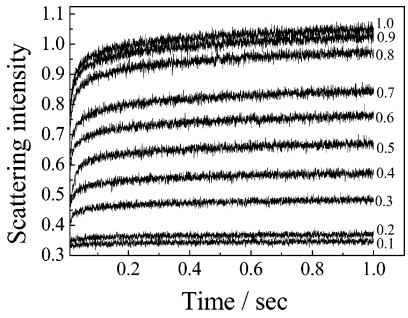

Figure 3. Time dependence of the scattering light intensity at different final concentrations (g/L) of $PEG_{113}-PGMA_{50}-PDEA_{65}$ triblock copolymer. The triblock copolymer solution was initially pH 3 and the final pH was 10.

$PDEA_{65}$ with x ranging from 0 to 50 mol %, the intensity-average hydrodynamic diameter, $\langle D_h \rangle$, was approximately 25 nm at pH 10, indicating that the esterification of the PGMA middle block had no significant effect on its micellization behavior, which is understandable considering that the water-solubility of the middle PGMA block is not compromised at the degrees of esterification targeted.

Parts a and b of Figure 2 show the ^{1}H NMR spectra recorded for the $PEG_{113}-(PCGMA_{0.5}\text{-}co\text{-}PGMA_{0.5})_{50}-PDEA_{65}$ triblock copolymer before shell cross-linking at pH 3 and 10, respectively. At pH 3, the copolymer chains are fully solvated, and all the signals expected for each block are visible. It should be noted that the NMR signals for the PCGMA block at δ 7.2−7.6 ppm and δ 6.4−6.6 ppm are clearly visible, confirming that the middle block is water-soluble even when the molar content of the CGMA residues in the middle block is 50 mol %. In contrast, the signals due to the PDEA block at δ 1.3 and 4.2 ppm completely disappeared at pH 10, while the signals for the PEG, PCGMA, and PGMA residues are still clearly evident, indicating the formation of the PDEA-core micelles with an inner shell comprising the water-soluble PGMA-*co*-PCGMA middle block and an outer corona of PEG chains.

Kinetic Studies of pH-Induced Micellization. The kinetics of the pH-induced micellization of $PEG_{113}-PGMA_{50}-PDEA_{65}$ and $PEG_{113}-(PCGMA_{0.5}\text{-}co\text{-}PGMA_{0.5})_{50}-PDEA_{65}$ was further investigated using stopped-flow techniques. For a pH jump from 3 to 10, each of the dynamic curves obtained for $PEG_{113}-PGMA_{50}-PDEA_{65}$ for concentrations ranging from 0.1 to 1.0 g/L exhibited positive amplitudes (see Figure 3), indicating micelle formation. The time dependence of the scattering light intensity, I_t, can be converted to a normalized function, namely $(I_\infty - I_t) / I_\infty$ vs t, where I_∞ is the value of I_t after an infinitely long

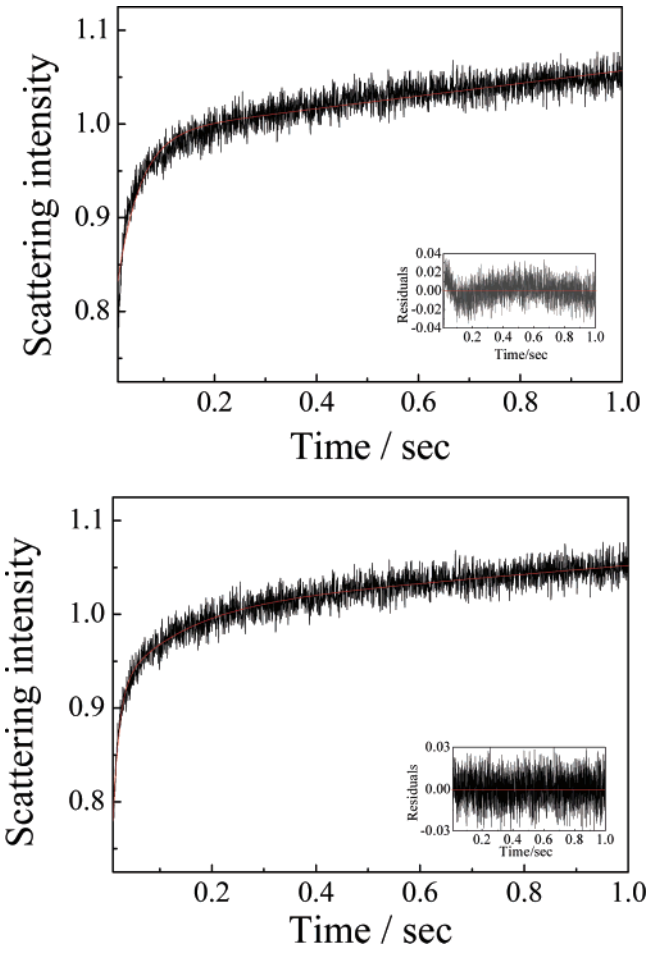

Figure 4. Typical time dependence of the scattering light intensity recorded during the micellar formation induced by a pH jump from 3 to 10. The upper and lower dynamic traces are fitted by single and double-exponential functions, respectively. The final concentration of the $PEG_{113}-PCGMA_{50}-PDEA_{65}$ copolymer was fixed at 1.0 g/L.

time. The relaxation curve cannot be adequately fitted using a single exponential function (see Figure 4a). This is particularly true for the first 0.2 s, which contains most of the useful kinetic information. Empirically, we found that the relaxation curve could be well-fitted by a double-exponential function (Figure 4b)

$$(I_\infty - I_t) / I_\infty = c_1 e^{-t/\tau_1} + c_2 e^{-t/\tau_2} \quad (1)$$

where c_1 and c_2 are the normalized amplitudes ($c_2 = 1 - c_1$), τ_1 and τ_2 are two characteristic relaxation times and $\tau_1 < \tau_2$. The mean micelle formation constant, τ_f, can be calculated as

$$\tau_f = c_1\tau_1 + c_2\tau_2 \quad (2)$$

Both τ_1 and τ_2 have positive amplitudes. All the dynamic curves shown in Figure 3 can be well-fitted with double-exponential functions. τ_1, τ_2, and the calculated parameter τ_f are shown in Figure 5a. For $PEG_{113}-PGMA_{50}-PDEA_{65}$, τ_1 is in the range of 10−15 ms, which decreases with increasing polymer concentration; τ_2 is ∼ 130 ms, which is almost independent of the copolymer concentration over the range studied.

Previously, we have studied the pH-induced micellization kinetics of poly(glycerol methacrylate)-*b*-poly(2-(dimethylamino)ethyl methacrylate)-*b*-poly(2-(diethylamino)ethyl methacrylate) (PGMA−PDMA−PDEA) triblock copolymer.[40] It seems that the pH-induced micellization kinetics of PEG−PGMA−PDEA is similar to that of PGMA−PDMA−PDEA. During the

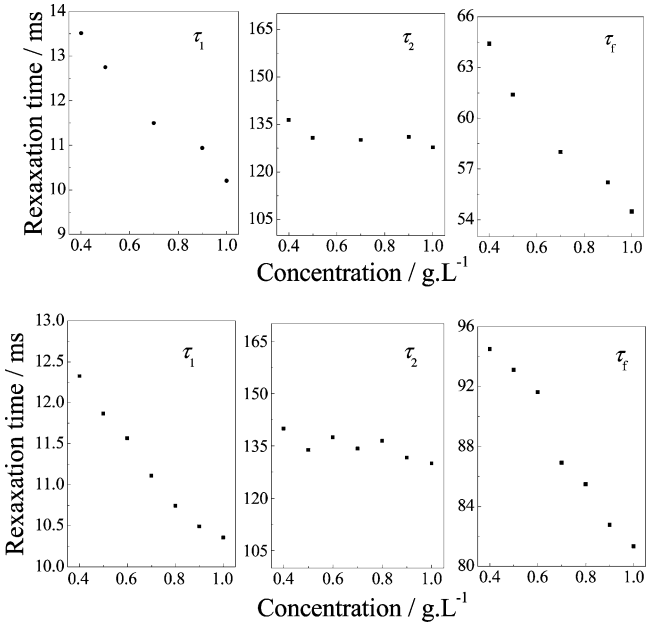

Figure 5. Double-exponential function fitting results obtained for micelle formation at varying concentrations of $PEG_{113}-PGMA_{50}-PDEA_{65}$ (top) and $PEG_{113}-(PCGMA_{0.5}\text{-}co\text{-}PGMA_{0.5})_{50}-PDEA_{65}$ (bottom) triblock copolymers. The experimental conditions are the same as in Figure 3.

unimer-to-micelle transition, the fast process (τ_1) is associated with the rapid association of unimers into quasi-equilibrium micelles; while the slow process (τ_2) is associated with micelle formation/breakup.

After formation of quasi-equilibrium micelles during the fast process, unimer concentration is supposed to be quite close to the critical micellization concentration (cmc). The relaxation from the quasi-equilibrium micelles to the final equilibrium micelles proceeds via micelle fusion/fission or unimer entry/expulsion.[41−43] Theoretical calculations[44] indicate that unimer exchange is faster than that of micellar fusion/fission at around the equilibrium state. Dormidontova et al.[41] also theoretically predicted that the characteristic time step required for the micelle fusion/fission mechanism in dilute solution is inversely proportional to the copolymer concentration, while for the unimer entry/expulsion mechanism, the characteristic relaxation time is almost independent of the copolymer concentration. The measured τ_2 for $PEG_{113}-PGMA_{50}-PDEA_{65}$ does not exhibit any concentration dependence; thus, it is reasonable to postulate that, during the slow process of micelle formation/breakup, unimer insertion/expulsion is the dominant mechanism for the relaxation from quasi-equilibrium micelles to the final equilibrium micelles.

Fitting results for all the dynamic curves obtained for the $PEG_{113}-(PCGMA_{0.5}\text{-}co\text{-}PGMA_{0.5})_{50}-PDEA_{65}$ triblock copolymer are shown in Figure 5b. It was found that typical relaxation times (τ_1, τ_2) for the micellization of the modified triblock copolymer are comparable to that of the $PEG_{113}-PGMA_{50}-PDEA_{65}$ triblock copolymer. This indicates that partial esterification of the PGMA block has negligible effects on the micellization kinetics.

The τ_f calculated from eq 2 for the overall micellization process ranges between 55 and 65 ms and 80−95 ms for the $PEG_{113}-PGMA_{50}-PDEA_{65}$ and the $PEG_{113}-(PCGMA_{0.5}\text{-}co\text{-}PGMA_{0.5})_{50}-PDEA_{65}$ triblock copolymers, respectively (see Figure 5). In both cases, τ_f decreases with increasing copolymer concentration. Closer examination of the fitting results indicates that the systematically larger τ_f values obtained for the micellization of $PEG_{113}-(PCGMA_{0.5}\text{-}co\text{-}PGMA_{0.5})_{50}-PDEA_{65}$ are due to the larger normalized amplitude, c_2. This perhaps reflects the fact that the introduction of cinnamate groups reduces the hydrophilicity of the middle block.

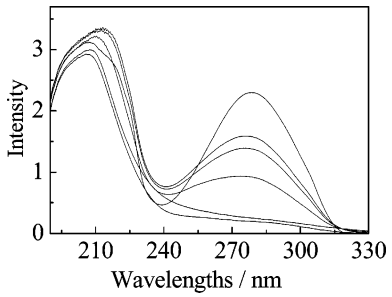

Figure 6. UV spectra of micellar solutions of $PEG_{113}-(PCGMA_{0.5}\text{-}co\text{-}PGMA_{0.5})_{50}-PDEA_{65}$ subjected to UV irradiation for 0, 1, 2, 5, 10, and 20 min (from top to bottom), where the triblock copolymer concentration is 1.0 g/L in each case.

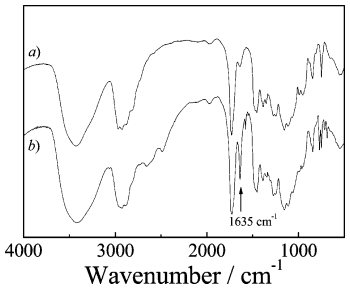

Figure 7. FT-IR spectra of the $PEG_{113}-(PCGMA_{0.5}\text{-}co\text{-}PGMA_{0.5})_{50}-DEA_{65}$ micelles after (a) and before (b) UV irradiation for 10 min at a copolymer concentration of 1.0 g/L.

Shell Cross-Linked Micelles with Responsive Cores. Upon UV irradiation, the double bonds of two neighboring cinnamate groups undergo photodimerization to produce a cyclobutane ring.[34] If two cinnamate groups on different copolymer chains dimerize, then interchain cross-linking reaction takes place.[45,46] Cross-linking of the PCGMA-*co*-PGMA inner shell within the PEG−(PCGMA-*co*-PGMA)−PDEA micelles was monitored by UV spectroscopy (see Figure 6). Longer irradiation times led to a reduction in the characteristic absorption peak at 274 nm, which is due to the cinnamate groups. After 10 min, the conversion of the cinnamate groups was ∼95%, with 98% conversion being achieved after UV irradiation for 20 min. Cross-linking was further confirmed by FT-IR spectroscopy. The absorption band at 1635 cm^{-1}, which is characteristic of the C═C stretch of the CGMA residues,[11,31,34] almost disappeared after 10 min UV irradiation (see Figure 7), while the intensity of the ester carbonyl band at 1730 cm^{-1} remained unchanged. The results shown in Figures 6 and 7 both indicate that the photo-cross-linking reaction of the CGMA units was almost complete after 10 min UV irradiation. Thus, to avoid possible UV-induced polymer degradation, UV irradiation for a duration of 10 min was always employed in subsequent photo-cross-linking reactions.

Assuming 100% photodimerization (which is approximately correct for 10 min UV irradiation), the molar contents of CGMA residues in the middle block were taken as the target degrees of cross-linking. It should be noted that the photodimerization of cinnamate groups can occur on the same copolymer chain or between adjacent copolymer chains. Only the latter situation leads to effective interchain cross-linking of the inner shell, since the former scenario only results in intrachain cross-linking. Thus, the degree of photodimerization monitored by UV or FT-IR spectroscopy only represents an upper limit for the actual degree

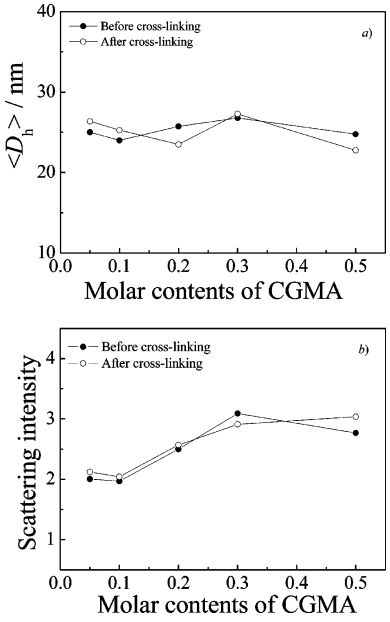

Figure 8. Variation of (a) $\langle D_h \rangle$ and (b) scattering intensities recorded before and after 10 min UV irradiation of an aqueous solution of 1.0 g/L $PEG_{113}-(PCGMA_x\text{-}co\text{-}PGMA_{1-x})_{50}-PDEA_{65}$ copolymer at pH 10 with different molar contents (x) of CGMA units in the middle block.

of cross-linking, which in principle can be tuned by adjusting the molar contents of CGMA units in the middle block.

Figure 8a shows the variation of the intensity-average hydrodynamic diameter, $\langle D_h \rangle$, for the $PEG_{113}-(PCGMA_x\text{-}co\text{-}PGMA_{1-x})_{50}-PDEA_{65}$ micelles before and after cross-linking at pH 10 as a function of the molar contents, x, of the CGMA units in the middle block. When x ranged from 0 to 50 mol %, the $\langle D_h \rangle$ of the non-cross-linked micelles is ~25 nm. After UV irradiation for ~10 min, the $\langle D_h \rangle$ of the SCL micelles remain unchanged. The polydispersity indexes (μ_2/Γ^2) of the micelles before and after cross-linking were also constant at around ~0.15. Figure 8b shows the variation of the scattering intensities of the non-cross-linked and cross-linked micelles as a function of x; no appreciable changes in scattering intensities can be detected. Both parts a and b of Figure 8 tell us that the cross-linking reaction takes place exclusively inside the inner layer and intermicellar cross-linking does not occur due to the steric repulsion imparted by the coronal PEG chains.[25,27] The above photo-cross-linking reaction was conducted at a concentration of 0.1 wt %, but similar results (i.e., no detectable intermicelle fusion) were also obtained at a copolymer concentration of 5.7 wt %. Dilution of the latter solution to 0.1 wt % led to colloidally stable micellar solutions with a characteristic bluish tinge, the $\langle D_h \rangle$ of these diluted SCL micelles is ~ 28 nm at pH 10, which is comparable to that prepared at much lower concentrations (25 nm for SCL micelles prepared at 0.1 wt % and pH 10).

Parts c and d of Figure 2 also show the ^1H NMR spectra recorded for the SCL micelles at pH 10 and 3, respectively. After UV irradiation for 10 min, the NMR signals of the double bonds of cinnamate groups at δ 6.5 ppm almost disappeared, again confirming that the photodimerization of the cinnamate groups is almost quantitative. When the solution pH of these SCL micelles was adjusted from 10 to 3 using DCl, the reappearance of signals assigned to the protonated DEA residues at δ 1.3 and 4.2 ppm again confirmed that the DEA cores of the SCL micelles were solvated and turned hydrophilic.

Figure 9 shows the swelling of the SCL micelles at acidic pH in terms of the shift of the hydrodynamic diameter distribution for $PEG_{113}-(PCGMA_{0.5}\text{-}co\text{-}PGMA_{0.5})_{50}-PDEA_{65}$

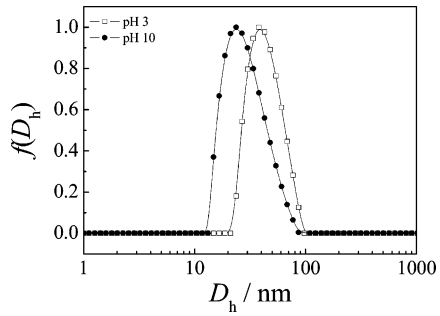

Figure 9. Typical hydrodynamic diameter distributions at pH 10 and pH 3 for the SCL micelles prepared from $PEG_{113}-(PCGMA_{0.5}\text{-}co\text{-}PGMA_{0.5})_{50}-PDEA_{65}$ triblock copolymer at 1.0 g/L.

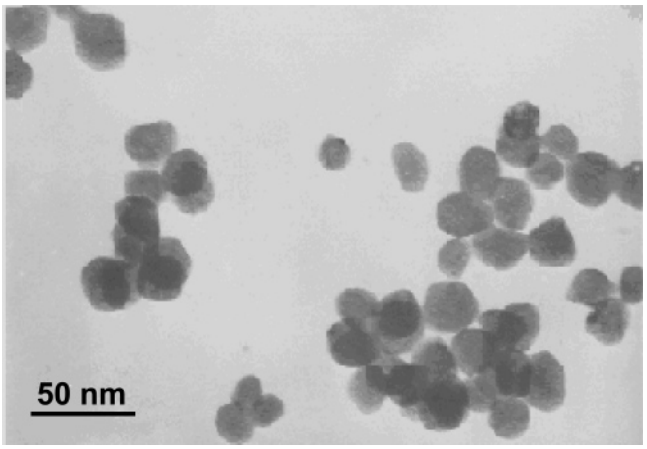

Figure 10. Typical TEM image obtained by drying an acidic solution (pH 3) of SCL micelles prepared using the $PEG_{113}-(PCGMA_{0.5}\text{-}co\text{-}PGMA_{0.5})_{50}-PDEA_{65}$ triblock copolymer.

triblock copolymer. At pH 10, the hydrodynamic diameter, D_h, of the SCL micelles ranged from 12 to 85 nm, with the peak located at ~24 nm. In contrast, D_h ranges from 20 to 100 nm at pH 3, with the peak located at 39 nm. The increase in size of the SCL micelles at low pH is due to the protonation and swelling of the PDEA cores at acidic pH. It should be noted that the swelling of the DEA cores is completely reversible: adjusting the solution pH back to 10 with NaOH led to the deswelling of the SCL micelles. TEM images of the SCL micelles dried at pH 3 (see Figure 10) revealed the presence of presumably spherical micelles of ~ 20−30 nm in diameter. Both the pH-induced swelling of the SCL micelles and the TEM studies indicated the successful shell cross-linking of the micelles. If the cross-linking had not been successful, the micelles would have dissociated into unimers and no spherical nanoparticles could be observed.

We also attempted the shell cross-linking of micelles from triblock copolymers with lower molar contents of CGMA units in the middle block. A series of $PEG_{113}-(PCGMA_x\text{-}co\text{-}PGMA_{1-x})_{50}-PDEA_{65}$ triblock copolymers with x ranging from 5 to 50 mol % was used for the preparation of micelles at pH 10 and then subjected to UV irradiation for 10 min. DLS was employed to detect the size change at pH 10 and 3 for the resulting SCL micelles (see Figure 11). We found that at $x =$ 5 and 10 mol %, the $\langle D_h \rangle$ measured at pH 10 is larger than that at pH 3. This suggests that the covalent stabilization of the micellar structure is not complete and that partial dissociation of the lightly cross-linked micelles occurs in acidic solutions. Figure 12 indicates that a minimum CGMA molar content of 20 mol % is required for the successful preparation of SCL

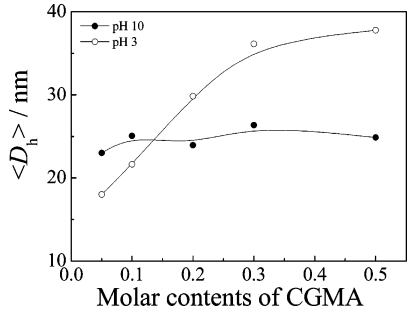

Figure 11. Variation of $\langle D_h \rangle$ as a function of the PCGMA molar contents for SCL micelles at both pH 3 and 10, respectively. The SCL micelles were prepared at 1.0 g/L and pH 10 by UV irradiation for 10 min.

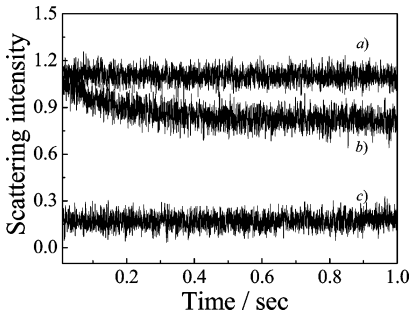

Figure 12. Time dependence of the scattering light intensities recorded for a pH jump from 10 to 3: (a) SCL micelles prepared from $PEG_{113}-(PCGMA_{0.5}\text{-}co\text{-}PGMA_{0.5})_{50}-PDEA_{65}$ triblock copolymer; (b) the SCL micelles prepared from the $PEG_{113}-(PCGMA_{0.2}\text{-}co\text{-}PGMA_{0.8})_{50}-PDEA_{65}$ triblock copolymer; (c) the non-cross-linked micelles of the $PEG_{113}-(PCGMA_{0.5}\text{-}co\text{-}PGMA_{0.5})_{50}-PDEA_{65}$ triblock copolymer. The final copolymer concentrations were fixed at 1.0 g/L in each case.

micelles under these conditions. Above this critical x value, the $\langle D_h \rangle$ of the SCL micelles at pH 3 is much larger than that at pH 10.

Stability of the Micelles before and after Shell Cross-Linking. The stability of the micelles before and after cross-linking was further examined by the stopped-flow technique (see Figure 12). For $PEG_{113}-(PCGMA_{0.5}\text{-}co\text{-}PGMA_{0.5})_{50}-PDEA_{65}$, the scattering intensities of the non-cross-linked micelles remain unchanged with time for a pH jump from 10 to 3 (see curve c). Compared to the scattering intensities of micelles at pH 10, it seems that the micelles completely dissociated into unimers within the dead time of the stopped-flow instrument (~3 ms for the stopped-flow setup used in these experiments). On the contrary, for the SCL micelles prepared from $PEG_{113}-(PCGMA_{0.5}\text{-}co\text{-}PGMA_{0.5})_{50}-PDEA_{65}$ obtained after UV irradiation for 10 min (see curve a), the scattering intensity for the same pH jump from 10 to 3 remains approximately constant with time, the absolute value is comparable to that obtained for the SCL micelles at pH 10, indicating the successful stabilization of the micellar structure. For SCL micelles prepared from $PEG_{113}-(PCGMA_{0.2}\text{-}co\text{-}PGMA_{0.8})_{50}-PDEA_{65}$ (see curve b), a pH jump from 10 to 3 lead to a gradual decrease in the scattering intensity for the first 0.5 s, suggesting that some triblock copolymer chains become detached from the SCL micelles within this time scale and that therefore cross-linking was not 100% complete in this case. This further supports the DLS results as shown in Figure 11. At pH 3, $\langle D_h \rangle$ of SCL micelles prepared from the copolymer at $x = 0.2$ is smaller that at $x = 0.5$. UV irradiation of micelles at $x = 0.2$ only leads to partial cross-linking of the micelles and some chains still exist un-cross-linked inside the micelles, although after cross-linking the micellar size at pH 3 is larger than that at pH 10. Stopped-flow technique thus proves to be a convenient technique for monitoring the extent of success in fixing the micellar structures and the kinetic process of free chains escaping from the SCL micelles after core solvating.

Conclusions

We have demonstrated a new facile approach for the preparation of the SCL micelles in aqueous solution from the PEG−(CGMA-*co*-GMA)−DEA micelles via UV irradiation-induced photo-cross-linking. The resulting SCL micelles exhibited reversible (de)swelling of the micellar cores on varying the solution pH. The effects of varying the molar contents of CGMA units in the middle block on the structural stability and pH-dependent (de)swelling of the SCL micelles were studied. The pH-induced micellization and dissociation kinetics for micelles before and after cross-linking were also investigated using the stopped-flow light scattering technique, which provides a convenient method for monitoring the extent of fixation of the micellar structures.

Acknowledgment. This work was supported by an Outstanding Youth Fund (Grant No. 50425310) and key research grants (Grant No. 20534020 and Grant No. 50233030) from the National Natural Scientific Foundation of China (NNSFC), the "Bai Ren" Project of the Chinese Academy of Sciences, and the Program for Changjiang Scholars and Innovative Research Team in University (PCSIRT). S.P.A. is a recipient of a 5-year Royal Society-Wolfson Research Merit award and also thanks EPSRC for a Platform Grant. Cognis Performance Chemicals are also thanked for donation of the GMA monomer.

References and Notes

(1) Thurmond, K. B.; Kowalewski, T.; Wooley, K. L. *J. Am. Chem. Soc.* **1996**, *118*, 7239.
(2) Karen, L. W. *J. Polym. Sci., Part A: Polym. Chem.* **2000**, *38*, 1397.
(3) Thurmond, K. B.; Kowalewski, T.; Wooley, K. L. *J. Am. Chem. Soc.* **1997**, *119*, 6656.
(4) Huang, H. Y.; Remsen, E. E.; Kowalewski, T.; Wooley, K. L. *J. Am. Chem. Soc.* **1999,** *121*, 3805.
(5) Ma, Q. G.; Remsen, E. E.; Kowalewski, T.; Wooley, K. L. *J. Am. Chem. Soc.* **2001**, *123*, 4627.
(6) Sanji, T.; Nakatsuka, Y.; Kitayama, F.; Sakurai, H. *Chem. Commun.* **1999**, 2201.
(7) Sanji, T.; Nakatsuka, Y.; Ohnishi, S.; Sakurai, H. *Macromolecules* **2000**, *33*, 8524.
(8) Ma, Q. G.; Wooley, K. L. *J. Polym. Sci., Part A: Polym. Chem.* **2000**, *38*, 4805.
(9) Underhill, R. S.; Liu, G. *Chem. Mater.* **2000**, *12*, 2082.
(10) Zhang, Q.; Remsen, E. E.; Wooley, K. L. *J. Am. Chem. Soc.* **2000**, *122*, 3642.
(11) Ding, J.; Liu, G. *J. Phys. Chem. B* **1998**, *102*, 6107.
(12) Ma, Q. G.; Remsen, E. E.; Kowalewski, T.; Schaefer, J.; Wooley, K. L. *Nano Lett.* **2001**, *1*, 651.
(13) Butun, V.; Billingham, N. C.; Armes, S. P. *J. Am. Chem. Soc.* **1998**, *120*, 12135.
(14) Butun, V.; Lowe, A. B.; Billingham, N. C.; Armes, S. P. *J. Am. Chem. Soc.* **1999**, *121*, 4288.
(15) Zhang, Z.; Liu, G.; Bell, S. *Macromolecules* **2000**, *33*, 7877.
(16) Wang, J. S.; Matyjaszewski, K. *Macromolecules* **1995**, *28*, 7901.
(17) Matyjaszewski, K.; Xia, J. *Chem. Rev.* **2001**, *101*, 2921.
(18) Wang, X. S.; Lascelles, S. F.; Jackson, R. A.; Armes, S. P. *Chem. Commun.* **1999**, 1817.
(19) Wang, X. S.; Jackson, R. A.; Armes, S. P. *Macromolecules* **2000**, *33*, 255.
(20) Wang, X. S.; Armes, S. P. *Macromolecules* **2000**, *33*, 6640.
(21) Liu, S. Y.; Weaver, J. V. M.; Tang, Y. Q.; Billingham, N. C.; Armes, S. P.; Tribe, K. *Macromolecules* **2002**, *35*, 6121.
(22) Robinson, K. L.; de Paz-Banez, M. V.; Wang, X. S.; Armes, S. P. *Macromolecules* **2001**, *34*, 5799.
(23) Save, M.; Weaver, J. V. M.; Armes, S. P.; McKenna, P. *Macromolecules* **2002,** *35*, 1152.

(24) Lobb, E. J.; Ma, I.; Billingham, N. C.; Armes, S. P.; Lewis, A. L. *J. Am. Chem. Soc.* **2001,** *123*, 7913.
(25) Liu, S. Y.; Weaver, J. V. M.; Save, M.; Armes, S. P. *Langmuir* **2002**, *18*, 8350.
(26) Liu, S. Y.; Armes, S. P. *Angew. Chem., Int. Ed.* **2002,** *41*, 1413.
(27) Butun, V.; Wang, X. S.; Banez, M. V. D.; Robinson, K. L.; Billingham, N. C.; Armes, S. P.; Tuzar, Z. *Macromolecules* **2000**, *33*, 1.
(28) Li, Y.; Lokitz, B. S.; McCormick, C. L. *Macromolecules* **2006**, *39*, 81.
(29) Li, Y.; Lokitz, B. S.; Armes, S. P.; McCormick, C. L. *Macromolecules* **2006**, *39*, 2726.
(30) Fujii, S.; Cai, Y. L.; Weaver, J. V. M.; Armes, S. P. *J. Am. Chem. Soc.* **2005**, *127*, 7304.
(31) Liu, F.; Liu, G. *Macromolecules* **2001**, *34*, 1302.
(32) Butun, V.; Top, R. B.; Ufuklar, S. *Macromolecules* **2006**, *39*, 1216.
(33) Pilon, L. N.; Armes, S. P.; Findlay, P.; Rannard, S. P. *Langmuir* **2005**, *21*, 3808.
(34) Guo, A.; Liu, G.; Tao, J. *Macromolecules* **1996**, *29*, 2487.
(35) Butun, V.; Billingham, N. C.; Armes, S. P. *Chem. Commun.* **1997**, 671.
(36) Lee, A. S.; Gast, A. P.; Butun, V.; Armes, S. P. *Macromolecules* **1999**, *32*, 4302.
(37) Butun, V.; Armes, S. P.; Billingham, N. C. *Polymer* **2001**, *42*, 5993.
(38) Vamvakaki, M.; Billingham, N. C.; Armes, S. P. *Macromolecules* **1999**, *32*, 2088.
(39) Zheng, Y.; Andreopoulos, F. M.; Micic, M.; Huo, Q.; Pham, S. M.; Leblanc, R. M. *Adv. Funct.* Mater. **2001**, *11*, 37.
(40) Zhu, Z.; Armes, S. P.; Liu, S. *Macromolecules* **2005**, *38*, 9803.
(41) Esselink, F. J.; Dormidontova, E.; Hadziioannou, G. *Macromolecules* **1998**, *31*, 2925.
(42) Esselink, F. J.; Dormidontova, E. E.; Hadziioannou, G. *Macromolecules* **1998**, *31*, 4873.
(43) Dormidontova, E. E. *Macromolecules* **1999**, *32*, 7630.
(44) Haliloglu, T.; Bahar, I.; Erman, B.; Mattice, W. L. *Macromolecules* **1996**, *29*, 4764.
(45) Yasuhide Nakayama, T. M. *J. Polym. Sci., Part A: Polym. Chem.* **1992**, *30*, 2451.
(46) Yasuhide Nakayama, T. M. *J. Polym. Sci., Part A: Polym. Chem.* **1993**, *31*, 977.

MA061386M